



Mixotrophic co-utilization of glucose and carbon monoxide boosts ethanol and butanol productivity of continuous *Clostridium carboxidivorans* cultures

Charlotte Anne Vees^a, Christoph Herwig^{a,b}, Stefan Pflügl^{a,*}

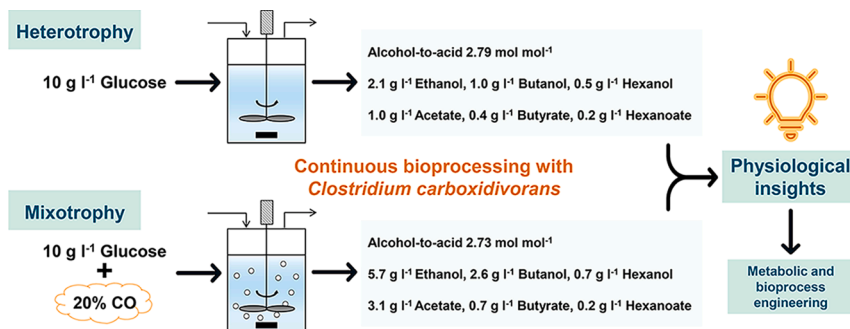
^a Technische Universität Wien, Institute of Chemical, Environmental and Bioscience Engineering, Research Area Biochemical Engineering, Gumpendorfer Straße 1a, 1060 Vienna, Austria

^b Competence Center CHASE GmbH, Altenbergerstraße 69, 4040 Linz, Austria

HIGHLIGHTS

- Optimal physiological operation of chemostats at 37 °C, pH 6 and 10 g l⁻¹ glucose.
- Continuous glucose cultivations show highest alcohol yield (0.39 Cmol Cmol⁻¹)
- Highest continuous butanol (2.6 g l⁻¹) and hexanol (0.7 g l⁻¹) production titers.
- Possible thermodynamic regulation of alcohol selectivity and chain elongation.
- Long-term glucose cultivations show shift to acid production (1.4 g l⁻¹ hexanoate)

GRAPHICAL ABSTRACT



ARTICLE INFO

Keywords:

Continuous chemostats
Acetogens
Mixotrophic gas fermentation
Carbon and energy efficiency
Metabolic modelling and thermodynamics

ABSTRACT

In this study, continuous cultivations of *C. carboxidivorans* to study heterotrophic and mixotrophic conversion of glucose and H₂, CO₂, and CO were established. Glucose fermentations at pH 6 showed a high ratio of alcohol-to-acid production of 2.79 mol mol⁻¹. While H₂ or CO₂ were not utilized together with glucose, CO feeding drastically increased the combined alcohol titer to 9.1 g l⁻¹. Specifically, CO enhanced acetate (1.9-fold) and ethanol (1.7-fold) production and triggered chain elongation to butanol (1.5-fold) production but did not change the alcohol:acid ratio. Flux balance analysis showed that CO served both as a carbon and energy source, and CO mixotrophy displayed a carbon and energy efficiency of 45 and 77%, respectively. This study expands the knowledge on physiology and metabolism of *C. carboxidivorans* and can serve as the starting point for rational engineering and process intensification to establish efficient production of alcohols and acids from carbon waste.

1. Introduction

Efficient bioproduction systems will be crucial for transitioning industrial production of value-added chemicals and fuels towards carbon

neutrality. Microbial fermentations have traditionally relied on starch-derived sugars as feedstocks. Nevertheless, gaseous feedstocks (CO₂, CO and H₂) have recently attracted attention as platform feedstocks of future circular bioeconomies (Köpke and Simpson, 2020). Currently

* Corresponding author.

E-mail addresses: charlotte.vees@tuwien.ac.at (C.A. Vees), christoph.herwig@tuwien.ac.at (C. Herwig), stefan.pflugl@tuwien.ac.at (S. Pflügl).

<https://doi.org/10.1016/j.biortech.2022.127138>

Received 8 March 2022; Received in revised form 5 April 2022; Accepted 6 April 2022

Available online 8 April 2022

0960-8524/© 2022 The Authors. Published by Elsevier Ltd. This is an open access article under the CC BY-NC-ND license (<http://creativecommons.org/licenses/by-nc-nd/4.0/>).

available from large industrial point sources or concentrated directly from air in the future, CO₂ and renewable energy can be used for electrochemical production of gaseous (syngas) and liquid (formate, methanol) (Cotton et al., 2020; Haas et al., 2018; Schreiber et al., 2020). In this context, acetogens are promising microbial hosts capable of utilizing these one carbon compounds to produce bulk chemicals such as organic acids and alcohols (Pavan et al., 2022). Acetogens utilize one-carbon compounds via the Wood-Ljungdahl pathway (WLP), the most energy-efficient of the currently known seven natural CO₂ fixation pathways (Veas et al., 2020).

Clostridium carboxidivorans P7 utilizes multiple hexoses and pentoses and is the only known acetogen to produce C4 and C6 acids and alcohols solely from gaseous feedstocks (Liou et al., 2005; Phillips et al., 2015; Rückel et al., 2021). Previous research with *C. carboxidivorans* has been focused on alcohol production via gas fermentation (Benevenuti et al., 2021; Doll et al., 2018; Fernández-Naveira et al., 2016; Kottenhahn et al., 2021; Riegler et al., 2019), where media composition (Phillips et al., 2015; Shen et al., 2017a; Zhang et al., 2016), pH range (Fernández-Naveira et al., 2017a), temperature (Kottenhahn et al., 2021; Ramió-Pujol et al., 2015; Shen et al., 2020), gas impurities (Rückel et al., 2021) and bioprocessing and reactor design (Abubackar et al., 2018; Doll et al., 2018; Riegler et al., 2019) have been investigated. Compared to gas fermentation, metabolism and physiology under heterotrophic conditions have received relatively little attention (Fernández-Naveira et al., 2017b; Kim et al., 2020; Li et al., 2021). Recent studies have improved the knowledge on pathways involved in metabolite synthesis but the lack of genome modification tools hamper in-depth physiological and metabolic analyses of *C. carboxidivorans* (Bruant et al., 2010; Cheng et al., 2019; Wirth and Dürre, 2021). Nevertheless, the factors regulating metabolism and governing selectivity of alcohol synthesis and chain elongation of metabolites in *C. carboxidivorans* are currently only poorly understood. Although *C. carboxidivorans* frequently produces mixtures of acetate/ethanol, butyrate/butanol and hexanoate/hexanol, the C2 compounds acetate and ethanol are usually the main products (C2 > C4 > C6) and high selectivity of alcohol production (i.e. high alcohol:acid ratios) has not been described. While the formation of reduced metabolites generally requires more reducing equivalents, chain elongation is bioenergetically less favorable compared to the formation of C2 compounds (Fast et al., 2015; Schuchmann and Müller, 2016). Bioenergetics play a key role in acetogen metabolism due to a limited amount of ATP which can be gained from growth on gaseous substrates (“life at the thermodynamic limit”) (Schuchmann and Müller, 2014). Mixotrophy, the simultaneous conversion of sugar and gaseous substrates, is an interesting concept in this context as it increases ATP production beyond levels for autotrophy and even heterotrophy (Fast et al., 2015; Jones et al., 2016; Schuchmann and Müller, 2016). In combination with gaseous electron donors to generate reducing power, mixotrophic sugar fermentations could potentially trigger alcohol synthesis and chain elongation. As such, mixotrophy has the potential to overcome limitations of sugar (carbon loss due to CO₂ production) and gas (low productivity and feedstock solubility in liquids) fermentations and could be used to implement flexible, highly efficient production platforms. Despite multiple examples of mixotrophic utilization of sugars and gases in acetogens (Braun and Gottschalk, 1981; Jones et al., 2016; Maru et al., 2018), no quantitative data on mixotrophy metabolism and physiology of *C. carboxidivorans* are available. Therefore, this study used continuous chemostat cultivations to investigate the metabolic response of *C. carboxidivorans* under heterotrophic and mixotrophic conditions. Quantitative physiological insights gained from heterotrophic glucose fermentations served as the reference point for comparison of different mixotrophic cultivation modes. Specifically, single gases and gas mixtures were co-fed in a well-controlled manner to get insights on the metabolic impact of additional carbon and energy sources on sugar fermentation. H₂, syngas and CO mixotrophic conditions were chosen and carbon and energy conversion efficiency, alcohol selectivity and formation of chain elongated metabolites were evaluated. Moreover, a

metabolic core model of *C. carboxidivorans* was established and used to analyze metabolic flux distributions and energy metabolism for heterotrophic and mixotrophic conditions. Based on the physiological data gained from the continuous cultivations of this study, potential thermodynamic and kinetic regulations of *C. carboxidivorans* metabolism are discussed.

2. Material and methods

2.1. Organism

Clostridium carboxidivorans P7 (DSM 15243) was used for all experiments in this study. The cells were stored as anoxic cryo culture at -80 °C in 37.5% (w/v) glycerol.

2.2. Growth media

The medium used for cultivation of *C. carboxidivorans* was a modified version of the medium described by Novak et al. (2021). The preculture medium contained per liter: 1 g NH₄Cl, 11.73 g KH₂PO₄, 2.406 g K₂HPO₄, 0.1 g MgSO₄ · 7H₂O, 2 g yeast extract, 0.194 mg Na₂SeO₃ · 5 H₂O, 0.192 mg Na₂WO₄ · 2 H₂O, 0.026 g FeSO₄ · 7 H₂O, 0.25 ml sodium resazurin (0.2% w/v), 0.5 g cysteine-HCl · H₂O, 5 g glucose, 20 ml trace element solution, and 10 ml vitamin solution. The medium was adjusted to pH 6.0 with 5 M KOH.

For bioreactor cultivations, the glucose concentration was increased to 10 g l⁻¹ or 20 g l⁻¹, while the phosphate buffer salts and sodium resazurin in the medium were reduced to 0.586 g l⁻¹ KH₂PO₄, 0.12 g l⁻¹ K₂HPO₄ and 0.20 ml l⁻¹, respectively.

The trace element solution contained per liter: 1.5 g nitrilotriacetic acid, 3 g MgSO₄ · 7 H₂O, 0.5 g MnSO₄ · H₂O, 1 g NaCl, 0.1 g FeSO₄ · 7 H₂O, 0.152 g Co(II)Cl₂ · 6 H₂O, 0.1 g CaCl₂ · 2 H₂O, 0.18 g ZnSO₄ · 7 H₂O, 0.01 g CuSO₄ · 5 H₂O, 0.02 g KAl(SO₄)₂ · 12 H₂O, 0.01 g H₃BO₃, 0.01 g Na₂MoO₄ · 2 H₂O, 0.033 g Ni(II)SO₄ · 6 H₂O, 0.3 mg Na₂SeO₃ · 5 H₂O and 0.4 mg Na₂WO₄ · 2 H₂O.

The vitamin solution contained per liter: 2 mg biotin, 2 mg folic acid, 10 mg pyridoxine-HCl, 5 mg thiamine-HCl, 5 mg riboflavin, 5 mg nicotinic acid, 5 mg D-Ca-pantothenate, 0.1 mg vitamin B12, 5 mg *para*-aminobenzoic acid and 5 mg lipoic acid.

Chemicals were purchased from Roth (Carl Roth GmbH + Co. KG, Karlsruhe, Germany) and Merck (Merck KGaA, Darmstadt, Germany).

2.3. Pre-culture preparation

For *C. carboxidivorans* pre-cultures, one cryo vial (1.8 ml) was used to inoculate one 125 ml serum bottle with 20 ml heterotrophic growth medium and incubated at 37 °C and 200 rpm (Infors AG, Bottmingen, Switzerland). After ~ 24 h, the culture was transferred anaerobically to fresh serum bottles (five per reactor) each with 40 ml medium, with an initial OD₆₀₀ of approximately 0.1 and incubated until the pH decreased to around 4.5. Afterwards, the pH was adjusted with 5 M NH₄OH to 5.5 to 6.0 and the culture incubated until the OD₆₀₀ reached 1.5. Using these exponentially growing cultures, bioreactors were inoculated with an initial OD₆₀₀ of approximately 0.2.

2.4. Cultivation in continuous bioreactors

The continuous bioreactor cultivations were carried out in 2-liter bioreactors (Applikon Biotechnology BV, Delft, Netherlands) with a working volume of 650 or 1000 ml. Cultivations were performed with a stirrer speed of 500 rpm and a temperature of 29 or 37 °C (as indicated). The pH was monitored by a pH electrode (Mettler-Toledo GmbH, Urdorf, Switzerland) and controlled by adding 6 M NH₄OH with a peristaltic pump (Cole-Parmer GmbH, Wertheim, Germany). Process control and monitoring were executed with a process information management system (Lucillus, Securecell AG, Urdorf, Switzerland).

To remove oxygen before inoculation, the reactor was sparged with 1 vvm nitrogen overnight. During cultivation the liquid medium was sparged with 0.25 vvm nitrogen or the respective gas mix. Pure nitrogen (Messer Austria GmbH, Gumpoldskirchen, Austria) was used during heterotrophic experiments. Gas mixtures were either premixed or blended by using pure gases. For the gas blends nitrogen was either mixed with hydrogen (60/40% (v/v) H₂/N₂) or carbon monoxide (20/80% (v/v) CO/N₂). H₂ and CO were obtained from Air Liquide Austria GmbH (Schwechat, Austria). Premixed gas with 60.1/9.5/10.6/19.8% (v/v) H₂/CO/CO₂/N₂ (Messer Austria GmbH, Gumpoldskirchen, Austria) was used to model industrial blast furnace gas blended with H₂. In this work, the gas mixture containing only H₂ was denoted as “H₂ mixotrophy” and the one containing only CO as “CO mixotrophy”. The ternary gas mix is denoted as “Syngas mixotrophy”. To enhance the gas transfer into the liquid, sinter metal microspargers (Sartorius Stedim Biotech GmbH, Göttingen, Germany) with 10 µm pore size were used. Gas flow rates were measured using a portable flow meter (Definer™ 220 Series, Mesa Laboratories, Butler/NJ, USA). The off-gas flow rate was monitored continuously during the cultivation. A two-stage cold trap was used to recover product stripped by gas flushing. Metabolite concentrations of the cold trap were included in the titer, rate and yield calculations.

For the continuous cultivation the feed medium and a 1:100 anti-foam solution (Polypropylenglycol P2000, Sigma-Aldrich, St. Louis, USA) were continuously pumped (Preciflow peristaltic pumps, Lambda Instruments GmbH, Baar, Switzerland) with a dilution rate of 0.05 h⁻¹ and 0.014 min⁻¹, respectively. A constant reactor volume was maintained by continuously harvesting culture broth through a dip tube by peristaltic pumps (Cole-Parmer GmbH, Wertheim, Germany).

To achieve steady state conditions the reactor volume was exchanged at least three times. Steady state was verified by checking for constant biomass, off-gas composition, and metabolite concentrations. Three samples for OD₆₀₀, CDW and HPLC determination were taken during steady state conditions in 3-hour intervals.

2.5. Optical density and biomass determination

The optical density at 600 nm (OD₆₀₀) was measured using a spectrophotometer (Genesys™20, Thermo Fisher Scientific, Waltham, USA).

The cell dry weight (CDW) was determined gravimetrically in triplicate. Briefly, 2 ml of the fresh culture was transferred into dried and pre-weighed glass tubes. The tubes were centrifuged, washed with 2 ml dH₂O, centrifuged again, followed by drying at 105 °C for at least 24 h. After cooling in a desiccator, the tubes were weighed and the cell dry weight calculated.

2.6. HPLC analysis

Glucose, organic acids, and alcohols in the liquid samples were analyzed with an Aminex HPX-87H column (300 × 7.8 mm, Bio-Rad, Hercules, USA) operated in an Ultimate 3000 HPLC system (Thermo Scientific, Waltham, USA). As mobile phase, 4 mM H₂SO₄ was used at a flow rate of 0.6 ml min⁻¹ and a column temperature of 60 °C. 10 µl samples were injected and 90 min chromatograms were recorded. For detection, a refractive index (Shodex RI-101, Showa Denko America, Inc., New York, USA) and a diode array detector (Ultimate 3000, Thermo Fisher Scientific, Waltham/MA, USA) were used.

HPLC samples were prepared by using 450 µl supernatant of the culture sample diluted with 50 µl of 0.04 M H₂SO₄ (Erian et al., 2018). The mixture was vortexed and centrifuged for 10 min at 14,000 rpm (21,913 g) at 4 °C. The supernatant was filled in HPLC vials. 5-point calibration curves were established by injecting 1 to 25 µl of standard solutions containing 1 to 6 g l⁻¹. Data analysis was done using Chromeleon 7.2.6 Chromatography Data System (Thermo Scientific, Waltham, USA).

2.7. Gas chromatography

To analyze H₂, CO, CO₂ and N₂ a gas chromatograph (Trace GC Ultra, Thermo Fisher Scientific, Waltham, USA) was used. 100 µl gas sample was automatically injected on a ShinCarbon ST 100/120 packed column (Restek Corporation, Bellefonte, USA) with a split ratio of 5 and a carrier gas flow of 2 ml min⁻¹ Argon 5.0 (Messer Austria, Gumpoldskirchen, Austria). The initial temperature of the column was 30 °C until 6.5 min and was increased to a temperature of 240 °C with a 16 °C min⁻¹ ramp and kept at 240 °C for 1.38 min. A thermal conductivity detector was used at 200 °C transfer, 240 °C block and 370 °C filament temperature to analyze the sample composition. An electronic multiplexing system was used to switch between the two reactors, allowing measurements to be done at one-hour intervals.

Data analysis was done using Chromeleon 7.2.10 Chromatography Data System (Thermo Scientific, Waltham, USA). Calibration was done using defined gas mixtures containing H₂, CO, CO₂ and N₂. Gas analysis of the gas feed to the reactor was done before and after cultivations. Off-gas was analyzed continually during the cultivation and at least four measurements were obtained per reactor once steady state conditions were reached.

2.8. Rate calculations, carbon and energy efficiency, and elemental balancing

For calculation of the volumetric rates of metabolite production and substrate uptake in the chemostat, the average concentrations from at least 3 data points obtained from steady state conditions were multiplied with the liquid dilution rate (D). The volumetric gas rates were calculated from the GC data as described by Neuendorf et al. (2021). Specific production and uptake rates were obtained by dividing the volumetric rates by the average biomass concentration. Yields (Y_{P/S}) in Cmol Cmol⁻¹ were calculated by dividing the volumetric production (P) of certain metabolite [Cmol l⁻¹ h⁻¹] by the sum of volumetric uptake (S) of glucose and CO [Cmol l⁻¹ h⁻¹].

Carbon efficiency was defined as the percentage of carbon retained in metabolites and biomass in relation to total carbon substrate turnover (glucose and CO) with the remaining carbon being released as CO₂. Calculations were performed using specific uptake and formation rates [Cmmol g⁻¹ h⁻¹] obtained from steady states.

Energy efficiency was defined as the energy retained in metabolites and biomass in relation to the energy supplied by the substrates (glucose, H₂, CO). Calculations were performed using the combustion energies of the individual compounds and their specific uptake and formation rates [mmol g⁻¹ h⁻¹].

For biomass, the average carbon content of 50% (w/w) was assumed for carbon balancing, while 4.20 mol electrons per mole of carbon were assumed for the degree of reduction (DoR) balance (Novak et al., 2021; Shen et al., 2020). All balances closed well without consideration of yeast extract.

2.9. Metabolic modeling and flux balance analysis

A metabolic core model of *C. carboxidivorans* was established based on a model available for *A. woodii* (Neuendorf et al., 2021; Novak et al., 2021) consisting of 139 reactions and 134 metabolites. The metabolic network, including substrate uptake, metabolite formation, energy conservation and redox balancing was implemented (see [supplementary material](#)). A biomass composition similar to *C. autoethanogenum* was assumed (Valgepea et al., 2017). Simulation of flux balance analysis (FBA) was done by using the CellNetAnalyzer toolbox (Klamt et al., 2007; von Kamp et al., 2017). Experimental rates for biomass formation, substrate uptake and metabolite formation were used to constrain the model. For simulations, the specific growth rate was kept constant (as data were obtained from steady state chemostat cultivations with a constant dilution rate D). Instead, the pseudo reaction that quantifies the

non-growth associated ATP maintenance (NGAM) demand served as objective function was maximized during FBA simulations. In this way, the intracellular flux distribution, and the upper limit of ATP available for NGAM processes were determined.

3. Results and discussion

3.1. Design and implementation of continuous glucose fermentations in *C. carboxidivorans*

Although earlier studies described glucose fermentation in batch cultures, continuous heterotrophic cultures of *C. carboxidivorans* utilizing glucose had not been demonstrated. Therefore, the first step of this investigation was to implement robust and stable operation of glucose fermentation in chemostat mode.

Consequently, suitable cultivation parameters for the heterotrophic reference chemostat were evaluated (Table 1). With the aim of establishing carbon-limited cultivations with complete sugar degradation, the glucose concentration (10 g l⁻¹, 20 g l⁻¹) was tested in combination with the liquid dilution rate (0.05 h⁻¹, 0.10 h⁻¹). Initial experiments showed cell washout at higher dilution rates and incomplete substrate utilization when the glucose concentration was increased. To exclude potential limitations from other medium components, dynamic pulse experiments were used to study the effect of individual medium components on glucose fermentation in continuous cultivation (data not shown). Using medium containing increased concentrations of iron, selenium, and tungsten significantly improved the ability of *C. carboxidivorans* to utilize glucose in continuous cultivations.

Next, the impact of a lower pH on *C. carboxidivorans* physiology in heterotrophic chemostats was verified. Lowering the culture pH has previously been shown to shift product formation towards alcohol synthesis in batch fermentations of syngas by *C. carboxidivorans* (Fernández-Naveira et al., 2016). However, decreasing the culture pH from 6.0 to 5.5 even at the lowest dilution rate tested (0.05 h⁻¹) resulted in cell washout. Therefore, it appears that the maximum specific growth rate at pH 5.5 is low despite previous studies reporting the optimal pH of *C. carboxidivorans* between 5.0 and 7.0 (Liou et al., 2005). Previous experiments in serum bottles also confirmed this observation, showing a growth rate of < 0.01 h⁻¹ at pH values below 5.5. Regarding mass transfer, two gas flow rates were tested to determine if stripping of CO₂ by the gas flow from the reactor negatively affects fixation of CO₂ evolved during glycolysis in the WLP. The experiments showed no significant difference hence the higher flow rate was chosen for all experiments to ensure sufficient gas-liquid mass transfer for subsequent mixotrophic experiments.

Next, the impact of the cultivation temperature on continuous cultures of *C. carboxidivorans* was investigated. To that end, the temperature was lowered to 29 °C, where a stable, carbon-limited chemostat with complete glucose utilization could be established. Previous studies indicated enhanced alcohol production and a shift towards longer chain products in autotrophic serum bottles using syngas when the cultivation temperature was lowered to 29 °C or even 25 °C from 37 °C, the optimal

growth temperature of *C. carboxidivorans* (Ramió-Pujol et al., 2015; Shen et al., 2017a; Shen et al., 2020; Zhang et al., 2016). Additionally, a lower cultivation temperature was shown to prevent an issue related to *C. carboxidivorans* morphology, which is the formation of cell agglomerates and pellets (Shen et al., 2020), which have previously been reported (Kottenhahn et al., 2021; Shen et al., 2017a) and were also observed in this study.

At 29 °C, the total alcohol yield decreased by 29% compared to 37 °C (Table 2 and supplementary material). This observation contrasts with previous findings from batch studies which have observed increased alcohol formation at lower cultivation temperatures (Ramió-Pujol et al., 2015; Shen et al., 2020; Zhang et al., 2016). Conversely, decreased alcohol formation was also observed in electricity-enhanced mixotrophic batch cultivations with *C. carboxidivorans* carried out at 25 °C (Cheng et al., 2022). Based on these data, a decreased maximum specific growth rate at 29 °C seems unlikely as the reason for lower alcohol production. In the chemostat runs, the specific growth rate is defined by the dilution rate applied which was at a fixed value of 0.05 h⁻¹ for both temperatures. Additionally, the biomass yield was comparable for both temperatures (0.16–0.17 Cmol Cmol⁻¹) indicating that growth was not affected by the downshift in temperature. Therefore, a more detailed analysis is required to understand how the cultivation temperature affects cell physiology and metabolite formation.

Finally, stable carbon-limited heterotrophic chemostats of *C. carboxidivorans* were established using 10 g l⁻¹ glucose, a dilution rate of 0.05 h⁻¹, a gassing rate of 0.25 vvm, pH 6.0 and 37 °C. Under these conditions, chemostats showed a biomass concentration of 1.4 g l⁻¹, corresponding to a yield of 0.17 Cmol Cmol⁻¹ (Table 2). *C. carboxidivorans* utilized glucose at a cell-specific rate of 2.1 mmol g⁻¹ h⁻¹ (Table 3). The product spectrum observed is in line with previous reports for batch cultivations on glucose and included: acetate/ethanol, butyrate/butanol, hexanoate/hexanol and traces of formate and lactate (Table 2) (Fernández-Naveira et al., 2017b). Despite the neutral pH of 6.0, a high alcohol:acid ratio of 2.79 mol mol⁻¹ was observed with combined titers of 1.6 and 3.7 g l⁻¹ for acids and alcohols, respectively (Fig. 1A). Acetate was the preferred acid formed, as indicated by the acetate:butyrate:hexanoate molar ratio of 1.0:0.23:0.12. Similarly, ethanol was the dominant alcohol produced with an ethanol:butanol:hexanol molar ratio of 1.0:0.31:0.11. In terms of productivity, combined rates for acid and alcohol formation of rates 1.1 and 3.2 mmol l⁻¹ h⁻¹, respectively, were observed (Table 4). Moreover, the combined alcohol yield shows that nearly 40% of carbon was converted into ethanol, butanol and hexanol (0.39 Cmol Cmol⁻¹) which is the highest yield reported for *C. carboxidivorans* (see supplementary material). Generally, *C. carboxidivorans* displayed a high carbon efficiency of 78% when utilizing glucose with only 22% of carbon being released as CO₂ (Fig. 2).

During the investigation, a second physiological steady-state of *C. carboxidivorans* was observed only noticeable after an extended cultivation time of > 450 h. While for shorter cultivation times a high alcohol:acid molar ratio was observed (termed “high state”), a state favoring acid formation (termed “low state”) was observed for long cultivation times (Table 2). The low state showed a significantly

Table 1

Overview of the process design parameters evaluated for the stable carbon-limited continuous cultivation of *C. carboxidivorans* on heterotrophic substrate. The final parameters were used for all following chemostat experiments.

Parameter	Final	Tested	Results
Glucose [g l ⁻¹]	10	10 / 20	Incomplete glucose utilization at 20 g l ⁻¹
Dilution rate [h ⁻¹]	0.05	0.05 / 0.10	Cell washout at 0.10 h ⁻¹
pH	6.0	6.0 / 5.5	Cell washout at lower pH
Gas flow rate [vvm]	0.25	0.25 / 0.10	No effect of gas flow on CO ₂ stripping and product formation
Temperature [°C]	37	37 / 29	Decreased alcohol productivity at 29 °C
Metals and trace elements	FeSO ₄ , Na ₂ SeO ₃ , Na ₂ WO ₄	CaCl ₂ , FeSO ₄ , NaCl, Na ₂ SeO ₃ , Na ₂ WO ₄ , NiSO ₄ , ZnSO ₄	Increased alcohol productivity and glucose uptake with additional Fe, Se, and W

Table 2

Titer and yield of acids, alcohols, and biomass from steady-state chemostat cultivations of *C. carboxidivorans* on 10 g l⁻¹ glucose at 37 °C and 29 °C (pH 6.0, dilution rate 0.05 h⁻¹). High: metabolic state obtained after short term cultivation, low: metabolic state observed after long-term cultivation (>450 h) in continuous cultivation mode. Mean values and standard deviations were calculated from biological replicates (8 at "high", 37 °C, 3 at "low", 37 °C, 2 at 29 °C).

Temp. [°C]	State	Titer [g l ⁻¹]	Butyrate	Hexanoate	Ethanol	Butanol	Hexanol	CDW	Y _{P/S} [Cmol Cmol ⁻¹]	Acetate	Butyrate	Hexanoate	Ethanol	Butanol	Hexanol	CDW	Carbon balance [%]	DoR balance [%]
37	high	1.00 ± 0.15	0.35 ± 0.10	0.23 ± 0.12	2.06 ± 0.47	1.04 ± 0.55	0.55 ± 0.25	1.43 ± 0.13	0.10 ± 0.01	0.10 ± 0.01	0.05 ± 0.01	0.03 ± 0.02	0.26 ± 0.06	0.06 ± 0.02	0.07 ± 0.04	0.17 ± 0.02	99.6 ± 10.4	98.8 ± 14.9
	low	2.12 ± 0.31	0.94 ± 0.03	1.38 ± 0.13	0.27 ± 0.06	0.19 ± 0.02	0.57 ± 0.24	1.44 ± 0.27	0.21 ± 0.03	0.21 ± 0.01	0.13 ± 0.01	0.21 ± 0.02	0.03 ± 0.01	0.03 ± 0.01	0.03 ± 0.04	0.10 ± 0.07	0.18 ± 0.03	123.6 ± 6.9
29	high	0.95 ± 0.05	0.43 ± 0.04	0.40 ± 0.08	1.40 ± 0.09	0.27 ± 0.02	0.44 ± 0.05	1.36 ± 0.03	0.09 ± 0.00	0.09 ± 0.00	0.06 ± 0.00	0.06 ± 0.01	0.17 ± 0.01	0.04 ± 0.00	0.07 ± 0.01	0.16 ± 0.00	89.5 ± 4.3	85.8 ± 1.9

CDW: biomass cell dry weight, DoR: degree of reduction, Temp.: temperature, Y_{P/S}: metabolite yield.

increased combined acid concentration of 4.4 g l⁻¹, with a C2:C4:C6 molar ratio of 1:0.31:0.35. A shift towards the formation of long-chain acids was observed, which is also reflected by a 6-fold increase in hexanoate formation (1.4 g l⁻¹ and 0.21 Cmol Cmol⁻¹), whereas acetate and butyrate formation increased 2.0-fold and 2.7-fold, respectively (Table 2). Conversely, the combined alcohol yield decreased by 59% compared to the high state. Additionally, a higher portion of carbon was released as CO₂ during the low state (33%, see supplementary material), indicating metabolic rearrangements related to the shift in metabolite formation. Despite this shift in metabolite formation, no changes in strain morphology were observed and biomass concentrations and yields for both states were comparable (Table 2). A more detailed analysis on a systems level is required to understand how extended cultivation periods mediate changes in metabolism. Ultimately, such insights could serve as the basis to implement genetic and bioprocess engineering strategies to tailor scenarios for selective alcohol or long-chain acid production.

3.2. H₂ mixotrophy: Impact of an additional electron source on glucose fermentation

In this study, the feasibility to mixotrophically utilize different gases in combination with glucose and the potential impact of different mixotrophic modes on strain physiology and metabolite formation was evaluated. Specifically, it was investigated whether metabolism can be shifted towards the formation of alcohols or generation of longer chain products (C4-C6 acids and alcohols) in the presence of different gas mixtures. Based on the heterotrophic reference chemostat, three gas mixtures corresponding to three mixotrophic cultivation modes were selected by providing either additional electrons using H₂ (H₂ mixotrophy) or additional carbon and electrons using H₂, CO and CO₂ (Syngas mixotrophy) or CO alone (CO mixotrophy). For the first mixotrophic scenario, H₂ mixotrophy, it was hypothesized that H₂ as an additional electron source could either promote an increased carbon conversion efficiency by fixing CO₂ evolving from glycolysis or shift metabolite production towards more reduced products, i.e. alcohols. To that end, chemostats were established under the same conditions as for heterotrophic glucose fermentation and introduced H₂ via the gas stream. However, H₂ feeding showed no significant effect on metabolite, CO₂ and biomass production as no H₂ uptake was noticeable (Table 3, Table 4). As such, the overall carbon conversion efficiency was comparable to the heterotrophic cultivations (83.4%, Fig. 2). The apparent inability of *C. carboxidivorans* to utilize H₂ under these conditions could be due to carbon catabolite repression (CCR) (Fast et al., 2015). Utilization of glucose by *C. carboxidivorans* could therefore simply repress H₂ consumption. For acetogens, CCR has been shown to be strain specific with no rationale available to predict the ability to co-consume H₂ with sugars without experimental verification. While multiple strains have been shown to efficiently co-utilize sugars and gaseous substrates (*A. woodii*, *T. kivui*, *C. ljungdahlii*, *C. autoethanogenum*) for other acetogens H₂ uptake was not observed in the presence of sugar substrates (*C. aceticum*, *M. thermoacetica*) (Braun and Gottschalk, 1981; Huang et al., 2012; Jones et al., 2016; Neuendorf et al., 2021). Besides H₂ utilization in the presence of sugars, also continuous cultures of *C. carboxidivorans* provided with syngas mainly consumed CO with low or no H₂ uptake (Doll et al., 2018). In case of syngas, CO inhibition of hydrogenases as an explanation for the lack in H₂ consumption needs to be considered. However, as the cultivations were carried out under CO-limiting conditions, inhibition of CO seems rather unfeasible. Rather, it appears that the ability of *C. carboxidivorans* to utilize H₂ is generally low. This explanation is underlined by the fact that *C. carboxidivorans* naturally grows poorly also on H₂/CO₂ where all reduction equivalents must be generated from H₂ oxidation (Lakhssassi et al., 2020). Nevertheless, a more detailed biochemical and systems level analysis is required to gain a more comprehensive picture of H₂ metabolism in *C. carboxidivorans*.

Table 3

Specific rates obtained from steady-state chemostat runs of *C. carboxidivorans* (37 °C, pH 6.0, dilution rate 0.05 h⁻¹) with 10 g l⁻¹ glucose (heterotrophy) and co-feeding of gas mixtures (mixotrophy). Mean values and standard deviations were calculated from biological replicates (heterotrophy: 8 replicates with 1.43 g l⁻¹ biomass, H₂ mixotrophy: 2 replicates with 1.67 g l⁻¹ biomass, Syngas mixotrophy: 2 replicates with 1.71 g l⁻¹ biomass, CO mixotrophy: 3 replicates with 2.32 g l⁻¹ biomass).

Operation mode	q _s [mmol g ⁻¹ h ⁻¹]			q _p [mmol g ⁻¹ h ⁻¹]							
	Glucose	CO	H ₂	CO ₂	H ₂	Acetate	Butyrate	Hexanoate	Ethanol	Butanol	Hexanol
Heterotrophy	2.06	–	–	2.66	0.14	0.60	0.14	0.07	1.59	0.49	0.18
	± 0.27	–	–	± 0.44	± 0.17	± 0.15	± 0.04	± 0.03	± 0.40	± 0.26	± 0.08
H ₂ mixotrophy	1.83	–	1.76	2.10	–	0.46	0.09	0.05	1.41	0.20	0.13
	± 0.41	–	± 1.19	± 0.62	–	± 0.15	± 0.00	± 0.02	± 0.74	± 0.05	± 0.02
Syngas mixotrophy	1.66	9.66	0.53	5.88	–	2.18	0.31	0.23	2.42	0.15	0.11
	± 0.01	± 2.37	± 0.37	± 0.44	–	± 0.40	± 0.22	± 0.02	± 0.16	± 0.22	± 0.01
CO mixotrophy	1.27	24.48	–	17.27	0.02	1.12	0.16	0.03	2.69	0.74	0.15
	± 0.20	± 2.72	–	± 1.56	± 0.01	± 0.32	± 0.02	± 0.01	± 0.50	± 0.09	± 0.05

q_s: specific uptake rate (glucose, CO, H₂), q_p: specific production rate (metabolites, CO₂, H₂).

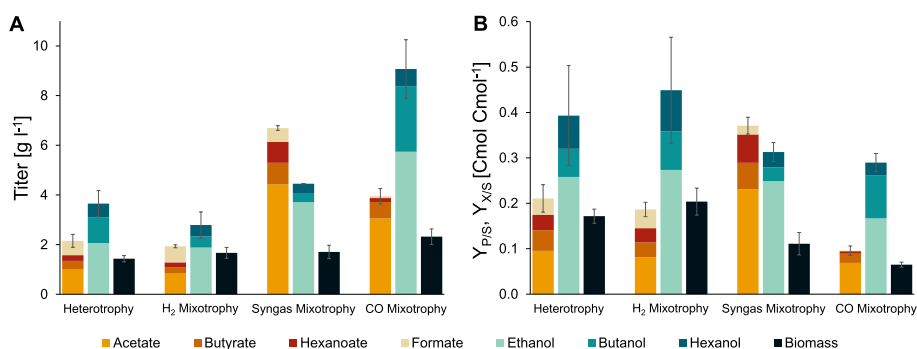


Fig. 1. Comparison of heterotrophic and mixotrophic titers (A) and yields (B) of *C. carboxidivorans* chemostat cultivations (cultivation conditions: 37 °C, pH 6.0, dilution rate 0.05 h⁻¹). Mean values and standard deviations were calculated from biological replicates (heterotrophy: 8, Syngas and H₂ mixotrophy: 2, CO mixotrophy: 3). Titer is given in g l⁻¹, yield is given in Cmol per Cmol glucose and CO.

Table 4

Volumetric rates obtained from steady-state chemostat runs of *C. carboxidivorans* (37 °C, pH 6.0, dilution rate 0.05 h⁻¹) with 10 g l⁻¹ glucose (heterotrophy) and co-feeding of gas mixtures (mixotrophy). Mean values and standard deviations were calculated from biological replicates (heterotrophy: 8, H₂ and Syngas mixotrophy: 2, CO mixotrophy: 3).

Operation mode	r _s [mmol l ⁻¹ h ⁻¹]			r _p [mmol l ⁻¹ h ⁻¹]								Carbon balance [%]	DoR balance [%]
	Glucose	CO	H ₂	CO ₂	H ₂	Acetate	Butyrate	Hexanoate	Ethanol	Butanol	Hexanol		
Heterotrophy	2.92	–	–	3.77	0.19	0.84	0.20	0.10	2.25	0.70	0.27	99.6	98.8
	± 0.16	–	–	± 0.46	± 0.22	± 0.15	± 0.06	± 0.05	± 0.50	± 0.36	± 0.12	10.4	14.9
H ₂ mixotrophy	2.97	–	2.68	3.38	–	0.73	0.14	0.09	2.18	0.32	0.22	103.3	107.5
	± 0.29	–	± 1.60	± 0.57	–	± 0.15	± 0.01	± 0.04	± 0.93	± 0.04	± 0.06	8.6	12.4
Syngas mixotrophy	2.84	15.87	0.81	10.04	–	3.84	0.47	0.33	4.10	0.25	0.18	109.9	129.2
	± 0.43	± 1.44	± 0.48	± 1.89	–	± 1.27	± 0.30	± 0.01	± 0.37	± 0.32	± 0.02	6.3	4.0
CO mixotrophy	2.90	56.14	–	39.94	0.03	2.53	0.37	0.07	6.17	1.75	0.33	99.1	97.7
	± 0.07	± 4.59	–	± 5.77	± 0.03	± 0.40	± 0.05	± 0.02	± 1.02	± 0.42	± 0.12	5.9	5.1

DoR: degree of reduction, r_s: volumetric uptake rate (glucose, CO, H₂), r_p: volumetric production rate (metabolites, CO₂, H₂).

3.3. Syngas mixotrophy: Impact of additional carbon and electron sources on glucose fermentation

Next, Syngas mixotrophy was studied, where in addition to H₂ also CO₂ and CO were supplied to continuous glucose cultivations. With the demonstrated ability of *C. carboxidivorans* to utilize CO, it was anticipated that co-utilization of glucose and syngas could trigger shifts in metabolism. Indeed, upon changing to a syngas gas feed, a specific CO uptake rate of 9.7 mmol g⁻¹ h⁻¹ was observed (Table 3). Similar to H₂ mixotrophic cultures and studies reporting autotrophic syngas fermentation at ambient pressure with *C. carboxidivorans*, no significant H₂ uptake was observed (Doll et al., 2018; Ramió-Pujol et al., 2015; Rückel et al., 2021; Shen et al., 2020). Nevertheless, *C. carboxidivorans* has been reported to grow on H₂/CO₂ (Lakhssassi et al., 2020; Liou et al., 2005) and that at least one of its hydrogenases is CO-tolerant (Schuchmann

et al., 2018). Moreover, H₂ consumption has been reported for growth on syngas in both serum bottles and bioreactor cultivations (operated at 2 bar) (Shen et al., 2017b). Therefore, H₂ utilization by *C. carboxidivorans* seems to be limited to conditions with high partial pressures, a crucial aspect to be considered for bioprocess development.

With the increased total carbon turnover resulting from CO consumption, also the steady state biomass concentration (+20%, Fig. 1A) increased. Consequently, the specific glucose uptake rate decreased (-20%, Table 3), as the total amount of glucose supplied to the culture remained constant. Additionally, significant changes in metabolite formation were observed. Specifically, the combined titers for acid and alcohol production increased 3.9-fold and 1.2-fold, respectively, when compared to heterotrophy (Fig. 1A). Considering that CO consumption boosts the carbon flux through the Wood-Ljungdahl pathway, additional acetyl-CoA appears to be preferably converted into acetate and ethanol

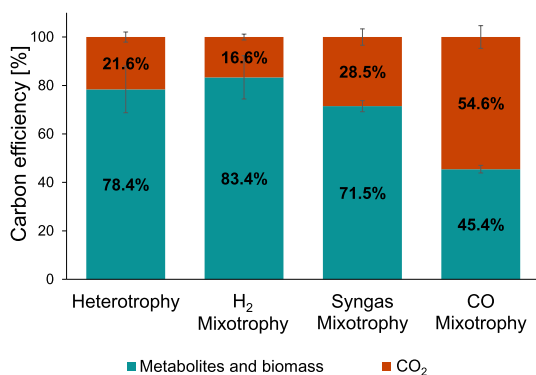


Fig. 2. Carbon efficiency of heterotrophic and mixotrophic chemostats of *C. carboxidivorans*. For comparison of carbon conversion efficiencies, carbon balances were set to 100% for each condition.

rather than being utilized for synthesis of longer chain metabolites. This observation is reflected by titers of 4.4 g l^{-1} (+342% compared to heterotrophy) and 3.7 g l^{-1} (+80% compared to heterotrophy) for acetate and ethanol (Fig. 1A), respectively. Additionally, the molar ratios for acids and alcohols reflect the preference for acetate and ethanol formation: 1.0:0.14:0.11 (acetate:butyrate:hexanoate) and 1.0:0.06:0.05 (ethanol:butanol:hexanol) (Table 3). Despite an overall enhanced acid (4-fold) and alcohol (1.4-fold) productivity (Table 4), total carbon conversion efficiency decreased to 71.5% (Fig. 2). Concomitantly, a 2.2-fold increased specific CO₂ evolution rate was observed, which reflects that CO is partially oxidized to CO₂ to serve as an electron source (by generation of reduced ferredoxin) and only partially as a carbon source (Table 3). Generally, CO₂ production rates from this study match well with reported values (9–50 mmol l⁻¹ h⁻¹, see supplementary material) for *C. carboxidivorans* (Doll et al., 2018; Riegler et al., 2019; Rückel et al., 2021) and other acetogens such as *C. autoethanogenum* and *C. ljungdahlii* (Hermann et al., 2020; Valgepea et al., 2018; Valgepea et al., 2017).

3.4. CO mixotrophy: Impact of enhanced CO supply on *C. carboxidivorans* metabolism

Based on the promising results from Syngas mixotrophy, i.e. increased formation of C₂ compounds by CO and glucose co-utilization, the next step was to investigate if an increased supply of CO can further boost alcohol productivity or trigger formation of longer chain elongation alcohols. The rationale behind this approach was that additional CO could increase the pool of acetyl-CoA (via enhanced activity of the WLP) available for chain elongation and at the same time provide Fd²⁻ (through partial oxidation to CO₂) needed for reduction of acids to their corresponding alcohols. To that end, CO was used as the sole gaseous carbon and electron source as H₂ and Syngas mixotrophy had not shown an effect of either H₂ or CO₂ on metabolite formation by *C. carboxidivorans*. Consequently, continuous glucose cultures were supplied with 20% CO in N₂. Doubling the amount of CO in the gas feed led to a 1.6-fold increase in biomass concentration compared to heterotrophy (Fig. 1A). Consequently, the specific glucose uptake rate decreased by 38% as the overall amount of glucose fed to the system remained constant (Table 3). In contrast, the specific CO uptake rate increased 2.5-fold to $24.5 \text{ mmol g}^{-1} \text{ h}^{-1}$ (Table 3), which is comparable to reported values of 29–42 mmol g⁻¹ h⁻¹ (Doll et al., 2018; Riegler et al., 2019; Rückel et al., 2021) for *C. carboxidivorans* (see supplementary material) and other acetogens (Hermann et al., 2020; Nagarajan et al., 2013; Valgepea et al., 2017). As a result of the increased CO uptake, CO mixotrophy was accompanied by a significant increase in CO₂ evolution. The specific CO₂ rate was $17.3 \text{ mmol g}^{-1} \text{ h}^{-1}$, 2.9-fold and 6.5-fold higher compared to Syngas mixotrophy and heterotrophy, respectively (Table 3). Consistent with the high specific CO₂ evolution rate, the

overall carbon efficiency decreased to 45.4% (Fig. 2). Reference values for carbon efficiency of *C. carboxidivorans* are scarce, with the notable exception of a recently published study investigating electricity-enhanced mixotrophy reporting a wide range of carbon efficiencies (53–83%) (Cheng et al., 2022). However, values similar to CO mixotrophy in *C. carboxidivorans* have been reported for autotrophic syngas and CO utilization by *C. ljungdahlii* and *C. autoethanogenum* (36–59%) (Hermann et al., 2020; Valgepea et al., 2018; Valgepea et al., 2017).

CO mixotrophy resulted in the highest metabolite titers of this study, with combined acid and alcohol titers of 3.9 g l^{-1} (+145% compared to heterotrophy) and 9.1 g l^{-1} (+148% compared to heterotrophy), respectively (Fig. 1A). Under these conditions, acetate, ethanol, and butanol were the major metabolites formed, with titers of 3.1, 5.7 and 2.6 g l^{-1} , respectively (Fig. 1A). Consequently, also the specific formation rates for acetate, ethanol, and butanol were enhanced 1.9, 1.7 and 1.5-fold, respectively, while the rates for butyrate, hexanoate and hexanol were comparable to the heterotrophic cultivation (Table 3). Overall, the molar alcohol:acid ratio was $2.73 \text{ mol mol}^{-1}$, comparable to $2.79 \text{ mol mol}^{-1}$ observed for heterotrophy. Despite higher production rates for acetate, ethanol, and butanol, the high oxidation rate of CO decreased the yield for acids and alcohols by 45% and 23%, respectively, compared to heterotrophy (Fig. 1B). Nevertheless, the alcohol yields for CO mixotrophy are comparable to previous reports and the yields obtained under heterotrophic conditions are overall the highest values reported for *C. carboxidivorans* (see supplementary material). Moreover, the butanol and hexanol titers for CO mixotrophy are the highest reported values for continuous cultivations and the total alcohol titer was only surpassed by studies using continuous packed-bed and biofilm reactors (Shen et al., 2014; Shen et al., 2017b). However, in addition to being difficult-to-operate (uncontrolled cell growth and decreasing viability) (Vees et al., 2020), these reports showed significantly lower alcohol productivities of 2.4–6.1 mmol l⁻¹ h⁻¹ (see supplementary material).

3.5. In silico analysis of *C. carboxidivorans* metabolism: CO uptake triggers metabolic rearrangements

Next, a stoichiometric core model was established based on the metabolic pathways currently known to operate in *C. carboxidivorans* (Fig. 3). This model was then used to analyze and compare intracellular flux distributions of heterotrophic and CO mixotrophic conditions. Using the specific uptake and production rates determined for both conditions and the specific growth rate set by the liquid dilution rates of the cultures (0.05 h^{-1}), flux balance analyses were performed for which maximizing the non-growth associated ATP maintenance energy served as the objective function.

Expectantly, the presence of CO triggered significant changes in intracellular flux distributions. Specifically, the glycolytic flux was 57% lower for CO mixotrophy compared to heterotrophy (Fig. 4). In contrast, the flux through the Wood-Ljungdahl pathway increased 23-fold when CO was utilized in addition to glucose. Furthermore, roughly 80% of CO taken up was initially oxidized to CO₂ to generate reduction power (Fd²⁻). The acetyl-CoA synthesis rate for CO mixotrophy obtained from FBA indicates that 35% of CO-derived carbon was ultimately fixed (total carbon efficiency of 45.4%, Fig. 4B). Previously reported carbon efficiencies from CO for autotrophic cultures of *C. carboxidivorans* ($q_{\text{CO}_2}/q_{\text{CO}} \sim 0.63\text{--}0.69$) and *C. autoethanogenum* ($q_{\text{CO}_2}/q_{\text{CO}} \sim 0.68$) closely match with the findings of this study ($q_{\text{CO}_2}/q_{\text{CO}} = 0.71$) (Doll et al., 2018; Valgepea et al., 2018). Based on this observation the carbon efficiency from CO in acetogenic hosts capable of synthesizing mixtures of more (alcohols) and less (acids) reduced metabolites appears to be constant and independent from the presence of other, high energy carbon sources such as glucose. In addition to the carbon efficiency, energetic efficiencies were calculated, i.e. the portion of energy from a substrate which is retained in the metabolites and biomass formed during fermentation. It was found that the energetic efficiency for CO

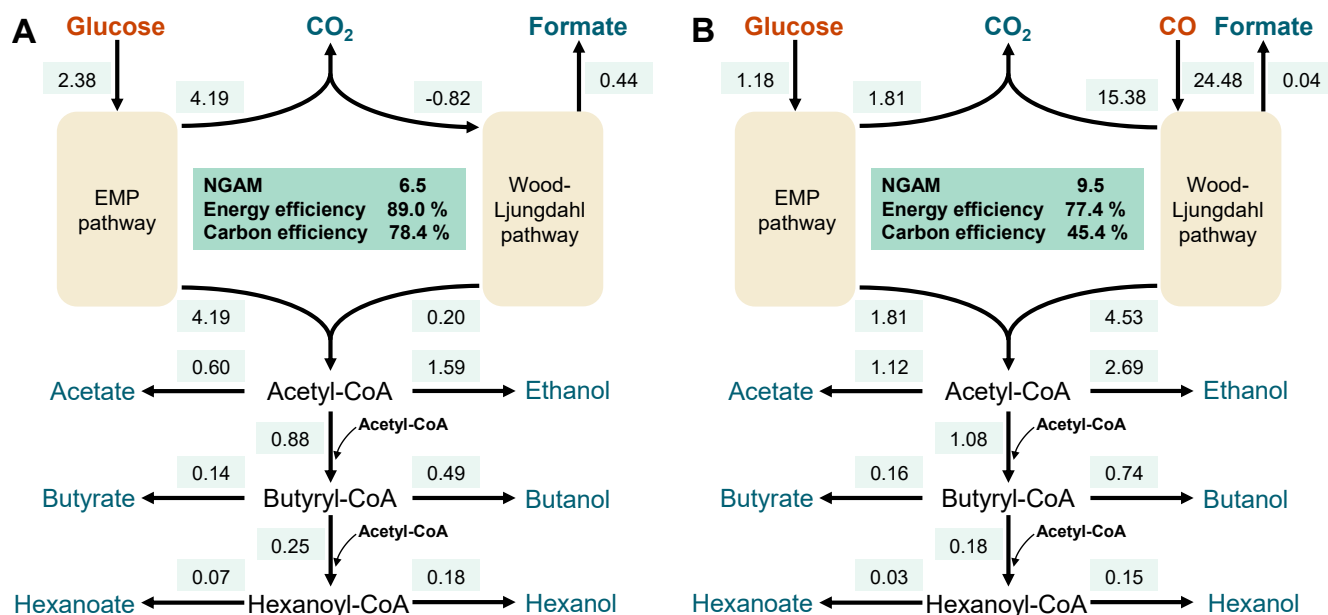


Fig. 4. Intracellular flux distributions of *C. carboxidivorans* for heterotrophic (A) and CO mixotrophic (B) chemostat cultivations. Flux values (light green boxes) are given in mmol g⁻¹ h⁻¹ and represent mean values of biological replicates (heterotrophy: 8, CO mixotrophy: 3). Central box (green) indicates non-growth associated ATP maintenance (NGAM, mmol g⁻¹ h⁻¹), energy and carbon efficiency. NGAM maximization was used as objective function for FBA simulations.

furthermore supported by the observation that significant portions of alcohols (~50%) were removed from the culture broth via gas stripping. As such, a higher thermodynamic driving force might have been achieved by efficient removal of the product of the 2-step conversion reaction (acid-aldehyde-alcohol). Despite results from *in silico* modeling and thermodynamic feasibility of the Aor route, it cannot be excluded that alcohol production at least partially occurs via the bioenergetically less favorable route for NADH-dependent reduction of acetyl-CoA to acetaldehyde. This reaction shows a $\Delta_rG \sim -20$ kJ mol⁻¹ (1 mM acetyl-CoA, 1 μ M acetaldehyde, pH 6.5), more exergonic than the Aor reaction under the same conditions.

In addition to stripping of products, lowering the culture pH is expected to increase alcohol selectivity. Specifically, at a culture pH of 5, an intracellular pH of 6, and an extracellular acetate titer of 3 g l⁻¹, the overall thermodynamic driving force for acetic acid ($\Delta_rG \sim -13$ kJ mol⁻¹ for 18 mM acetic acid) and acetate ($\Delta_rG \sim -10$ kJ mol⁻¹ for 317 mM acetate) significantly improves towards aldehyde and alcohol formation. However, all attempts to establish continuous cultures at a pH lower than 6 were unsuccessful. Likewise, 2-step continuous cultures with a pH of 6 and 5 in the first and second step, respectively, did not show growth and an overall low metabolic activity in the second stage (Doll et al., 2018). Therefore, batch cultivations are the only examples for *C. carboxidivorans* cultivated at a lower culture pH. Shifting pH from 5.75 to 4.75 after an initial phase of growth led to a shift in alcohol:acid ratio to 1.48 compared to cultures without a shift (0.30) (Fernández-Naveira et al., 2016). Consequently, continuous bioprocessing with high alcohol selectivity at low culture pH likely requires measures such as cell retention systems to maintain a high biocatalyst concentration and activity without the need for growth. Generally, an analysis on the proteomic and transcriptomic level in combination with metabolic modeling is required to verify thermodynamic and kinetic regulations as the trigger for alcohol synthesis.

Next to alcohol selectivity, chain elongation is the second dimension of metabolite formation in *C. carboxidivorans*. Under which conditions chain elongated products are formed remains largely unclear. Generally, formation of acids and alcohols followed a C2 > C4 > C6 pattern (Doll et al., 2018; Fernández-Naveira et al., 2017a; Shen et al., 2017a). As such, it appears likely that thermodynamics and kinetics are also

involved in the formation of metabolites beyond acetate and ethanol. Acetyl-CoA as the turntable of metabolism can either be used for acetate/ethanol formation via the Pta reaction (Δ_rG of 9.0 kJ mol⁻¹) or for chain elongation via the thiolase reaction (Δ_rG of 25 kJ mol⁻¹). Consequently, under standard conditions formation of C2 products is thermodynamically more favorable than chain elongation. FBA showed a 44% higher flux towards acetyl-CoA for CO mixotrophy compared to heterotrophy. Therefore, the moderate shift in the ethanol:butanol:hexanol towards butanol formation observed for the CO mixotrophy could be due to higher intracellular acetyl-CoA levels. However, a CO-grown continuous culture of *C. carboxidivorans* showed an even higher flux towards acetyl-CoA formation with only small amounts of butyrate and butanol formed. In this study, only CO mixotrophy showed increased levels of butanol. In addition to thermodynamic regulation by the acetyl-CoA pool, availability of ATP (provided by glucose and CO) and reducing power (mainly from CO) are potentially involved in regulating synthesis of longer chain products. Furthermore, feeding of surplus amounts of acetate and CO to a co-culture of *C. autoethanogenum* and *Clostridium kluyveri* has been shown to promote chain elongation (Diender et al., 2016). Consequently, metabolomics measurements to determine intracellular acetyl-CoA and ATP levels in combination with bioprocessing strategies supplying additional glucose, CO or acetate to modulate ATP, redox and acetyl-CoA household could be used to study regulation of chain elongation in *C. carboxidivorans*. Additionally, rational metabolic engineering could be extremely helpful in identifying metabolic regulations. However, the development of genetic tools has hitherto been hampered by the complex DNA restriction-modification system of *C. carboxidivorans* which prevents introducing foreign DNA effectively (Bourgade et al., 2021).

Despite the remaining challenges, the broad product spectrum, and its ability to utilize multiple pentoses and hexoses in addition to gaseous substrates render *C. carboxidivorans* a promising microbial host. Pushing mixotrophic processes towards industrial application, *C. carboxidivorans* could be used as a carbon- and energy-efficient bioproduction system for mixotrophic upgrading of low-cost sugar feedstocks such as spent sulfite liquor and industrial waste gas streams into value-added products.

4. Conclusion

In this study, heterotrophic and mixotrophic chemostats of *C. carboxidivorans* have been used to understand co-utilization of glucose and gaseous feedstocks. CO as a carbon and energy source was found to be efficiently co-utilized with glucose. CO mixotrophy displayed high alcohol titers and productivities. Mixotrophic conversion was also characterized by a high energetic efficiency. An *in silico* metabolic analysis showed that selectivity of alcohol production and chain elongation appear to be regulated on the thermodynamic and bioenergetic level. The physiological insights of this study therefore lay the foundation for establishing efficient alcohol production from waste streams in the future.

Funding

This work was supported by Austrian Research Promotion Agency [#876301].

Ethical approval

This article does not contain any studies with human participants or animals performed by any of the authors.

CRedit authorship contribution statement

Charlotte Anne Veas: Conceptualization, Validation, Investigation, Writing – original draft, Visualization. **Christoph Herwig:** Resources, Writing – review & editing, Supervision, Funding acquisition. **Stefan Pflügl:** Conceptualization, Writing – original draft, Resources, Supervision, Project administration, Funding acquisition.

Declaration of Competing Interest

The authors declare no competing interests.

Acknowledgements

The authors are indebted to Emina Zejnilovic, Klara Wögerbauer and Andrea Leibetseder for excellent technical assistance and Christian Simon Neuendorf and Katharina Novak for support with the GC system. The authors acknowledge TU Wien Bibliothek for financial support through its Open Access Funding Programme.

Appendix A. Supplementary data

Supplementary data to this article can be found online at <https://doi.org/10.1016/j.biortech.2022.127138>.

References

- Abubackar, H.N., Veiga, M.C., Kennes, C., 2018. Production of acids and alcohols from syngas in a two-stage continuous fermentation process. *Bioresour. Technol.* 253, 227–234.
- Benevenuti, C., Branco, M., do Nascimento-Correa, M., Botelho, A., Ferreira, T., Amaral, P., 2021. Residual gas for ethanol production by *Clostridium carboxidivorans* in a dual impeller stirred tank bioreactor (STBR). *Fermentation* 7 (3), 199.
- Bourgade, B., Minton, N.P., Islam, M.A., 2021. Genetic and metabolic engineering challenges of C1-gas fermenting acetogenic chassis organisms. *FEMS Microbiol. Rev.* 45 (2), 1–20.
- Braun, K., Gottschalk, G., 1981. Effect of molecular hydrogen and carbon dioxide on chemo-organotrophic growth of *Acetobacterium woodii* and *Clostridium acetium*. *Arch. Microbiol.* 128 (3), 294–298.
- Bruant, G., Lévesque, M.-J., Peter, C., Guiot, S.R., Masson, L., 2010. Genomic analysis of carbon monoxide utilization and butanol production by *Clostridium carboxidivorans* strain P7^T. *PLoS ONE* 5 (9), e13033.
- Cheng, C., Li, W., Lin, M., Yang, S.-T., 2019. Metabolic engineering of *Clostridium carboxidivorans* for enhanced ethanol and butanol production from syngas and glucose. *Bioresour. Technol.* 284, 415–423.

- Cheng, C., Shao, Y., Li, W., Liu, J., Liu, X., Zhao, Y., Li, X., Yang, S.-T., Xue, C., 2022. Electricity-enhanced anaerobic, non-photosynthetic mixotrophy by *Clostridium carboxidivorans* with increased carbon efficiency and alcohol production. *Energy Convers. Manage.* 252, 115118.
- Cotton, C.A., Claessens, N.J., Benito-Vaquero, S., Bar-Even, A., 2020. Renewable methanol and formate as microbial feedstocks. *Curr. Opin. Biotechnol.* 62, 168–180.
- Diender, M., Stams, A.J.M., Sousa, D.Z., 2016. Production of medium-chain fatty acids and higher alcohols by a synthetic co-culture grown on carbon monoxide or syngas. *Biotechnol. Biofuels* 9 (82).
- Doll, K., Rückel, A., Kämpf, P., Wende, M., Weuster-Botz, D., 2018. Two stirred-tank bioreactors in series enable continuous production of alcohols from carbon monoxide with *Clostridium carboxidivorans*. *Bioprocess. Biosyst. Eng.* 41 (10), 1403–1416.
- Erian, A.M., Gibisch, M., Pflügl, S., 2018. Engineered *E. coli* W enables efficient 2,3-butanediol production from glucose and sugar beet molasses using defined minimal medium as economic basis. *Microb. Cell. Fact.* 17 (1), 190.
- Fast, A.G., Schmidt, E.D., Jones, S.W., Tracy, B.P., 2015. Acetogenic mixotrophy: novel options for yield improvement in biofuels and biochemicals production. *Curr. Opin. Biotechnol.* 33, 60–72.
- Fernández-Naveira, Á., Abubackar, H.N., Veiga, M.C., Kennes, C., 2016. Efficient butanol-ethanol (B-E) production from carbon monoxide fermentation by *Clostridium carboxidivorans*. *Appl. Microbiol. Biotechnol.* 100 (7), 3361–3370.
- Fernández-Naveira, Á., Veiga, M.C., Kennes, C., 2017a. Effect of pH control on the anaerobic H-B-E fermentation of syngas in bioreactors. *J. Chem. Technol. Biotechnol.* 92 (6), 1178–1185.
- Fernández-Naveira, Á., Veiga, M.C., Kennes, C., 2017b. Glucose bioconversion profile in the syngas-metabolizing species *Clostridium carboxidivorans*. *Bioresour. Technol.* 244, 552–559.
- Haas, T., Krause, R., Weber, R., Demler, M., Schmid, G., 2018. Technical photosynthesis involving CO₂ electrolysis and fermentation. *Nat. Catal.* 1 (1), 32–39.
- Hermann, M., Teleki, A., Weitz, S., Niess, A., Freund, A., Bengelsdorf, F.R., Takors, R., 2020. Electron availability in CO₂, CO and H₂ mixtures constrains flux distribution, energy management and product formation in *Clostridium ljungdahlii*. *Microb. Biotechnol.* 13 (6), 1831–1846.
- Huang, H., Wang, S., Moll, J., Thauer, R.K., 2012. Electron bifurcation involved in the energy metabolism of the acetogenic bacterium *Moorella thermoacetica* growing on glucose or H₂ plus CO₂. *J. Bacteriol.* 194 (14), 3689–3699.
- Jones, S.W., Fast, A.G., Carlson, E.D., Wiedel, C.A., Au, J., Antoniewicz, M.R., Papoutsakis, E.T., Tracy, B.P., 2016. CO₂ fixation by anaerobic non-photosynthetic mixotrophy for improved carbon conversion. *Nat. Commun.* 7, 12800.
- Kim, J., Kim, J., Um, Y., Kim, K.H., 2020. Intracellular metabolite profiling and the evaluation of metabolite extraction solvents for *Clostridium carboxidivorans* fermenting carbon monoxide. *Process Biochem.* 89, 20–28.
- Klamt, S., Saez-Rodríguez, J., Gilles, E.D., 2007. Structural and functional analysis of cellular networks with *Cell NetAnalyzer*. *BMC Syst. Biol.* 1 (2).
- Köpke, M., Simpson, S.D., 2020. Pollution to products: recycling of ‘above ground’ carbon by gas fermentation. *Curr. Opin. Biotechnol.* 65, 180–189.
- Kottenhahn, P., Philipps, G., Jennewein, S., 2021. Hexanol biosynthesis from syngas by *Clostridium carboxidivorans* P7 – product toxicity, temperature dependence and *in situ* extraction. *Heliyon* 7 (8), e07732.
- Lakhssassi, N., Baharlouei, A., Meksem, J., Hamilton-Brehm, S.D., Lightfoot, D.A., Meksem, K., Liang, Y., 2020. EMS-induced mutagenesis of *Clostridium carboxidivorans* for increased atmospheric CO₂ reduction efficiency and solvent production. *Microorganisms* 8 (8), 1239.
- Li, X., Han, R., Bao, T., Osire, T., Zhang, X., Xu, M., Yang, T., Rao, Z., 2021. Citrulline deiminase pathway provides ATP and boosts growth of *Clostridium carboxidivorans* P7. *Biotechnol. Biofuels* 14 (204).
- Liou, J.S.C., Balkwill, D.L., Drake, G.R., Tanner, R.S., 2005. *Clostridium carboxidivorans* sp. nov., a solvent-producing clostridium isolated from an agricultural settling lagoon, and reclassification of the acetogen *Clostridium scatologenes* strain SL1 as *Clostridium drakei* sp. nov. *Int. J. Syst. Evol. Microbiol.* 55 (5), 2085–2091.
- Maru, B.T., Munasinghe, P.C., Gilary, H., Jones, S.W., Tracy, B.P., 2018. Fixation of CO₂ and CO on a diverse range of carbohydrates using anaerobic, non-photosynthetic mixotrophy. *FEMS Microbiol. Lett.* 365 (8), fny039.
- Mock, J., Zheng, Y., Mueller, A.P., Ly, S., Tran, L., Segovia, S., Nagaraju, S., Köpke, M., Dürre, P., Thauer, R.K., 2015. Energy conservation associated with ethanol formation from H₂ and CO₂ in *Clostridium autoethanogenum* involving electron bifurcation. *J. Bacteriol.* 197 (18), 2965–2980.
- Nagarajan, H., Sahin, M., Nogales, J., Latif, H., Lovley, D.R., Ebrahim, A., Zengler, K., 2013. Characterizing acetogenic metabolism using a genome-scale metabolic reconstruction of *Clostridium ljungdahlii*. *Microb. Cell. Fact.* 12 (118).
- Neuendorf, C.S., Vignolle, G.A., Dermitt, C., Tomin, T., Novak, K., Mach, R.L., Birner-Grünberger, R., Pflügl, S., 2021. A quantitative metabolic analysis reveals *Acetobacterium woodii* as a flexible and robust host for formate-based bioproduction. *Metab. Eng.* 68, 68–85.
- Novak, K., Neuendorf, C.S., Kofler, I., Kieberger, N., Klamt, S., Pflügl, S., 2021. Blending industrial blast furnace gas with H₂ enables *Acetobacterium woodii* to efficiently co-utilize CO, CO₂ and H₂. *Bioresour. Technol.* 323, 124573.
- Pavan, M., Reinmets, K., Garg, S., Mueller, A.P., Marcellin, E., Köpke, M., Valgepea, K., 2022. Advances in systems metabolic engineering of autotrophic carbon oxide-fixing biocatalysts towards a circular economy. *Metab. Eng.* 71, 117–141.
- Phillips, J.R., Atiyeh, H.K., Tanner, R.S., Torres, J.R., Saxena, J., Wilkins, M.R., Huhnke, R.L., 2015. Butanol and hexanol production in *Clostridium carboxidivorans* syngas fermentation: Medium development and culture techniques. *Bioresour. Technol.* 190, 114–121.

- Ramió-Pujol, S., Ganigué, R., Bañeras, L., Colprim, J., 2015. Incubation at 25 °C prevents acid crash and enhances alcohol production in *Clostridium carboxidivorans* P7. *Bioresour. Technol.* 192, 296–303.
- Riegler, P., Chrusciel, T., Mayer, A., Doll, K., Weuster-Botz, D., 2019. Reversible retrofitting of a stirred-tank bioreactor for gas-lift operation to perform synthesis gas fermentation studies. *Biochem. Eng. J.* 141, 89–101.
- Rückel, A., Hannemann, J., Maierhofer, C., Fuchs, A., Weuster-Botz, D., 2021. Studies on syngas fermentation with *Clostridium carboxidivorans* in stirred-tank reactors with defined gas impurities. *Front. Microbiol.* 12 (655390).
- Schreiber, A., Peschel, A., Hentschel, B., Zapp, P., 2020. Life Cycle Assessment of power-to-syngas: comparing high temperature co-electrolysis and steam methane reforming. *Front. Energy Res.* 8 (533850).
- Schuchmann, K., Chowdhury, N.P., Müller, V., 2018. Complex multimeric [FeFe] hydrogenases: biochemistry, physiology and new opportunities for the hydrogen economy. *Front. Microbiol.* 9, 2911.
- Schuchmann, K., Müller, V., 2014. Autotrophy at the thermodynamic limit of life: a model for energy conservation in acetogenic bacteria. *Nat. Rev. Microbiol.* 12 (12), 809–821.
- Schuchmann, K., Müller, V., 2016. Energetics and application of heterotrophy in acetogenic bacteria. *Appl. Environ. Microbiol.* 82 (14), 4056–4069.
- Shen, S., Gu, Y., Chai, C., Jiang, W., Zhuang, Y., Wang, Y., 2017a. Enhanced alcohol titre and ratio in carbon monoxide-rich off-gas fermentation of *Clostridium carboxidivorans* through combination of trace metals optimization with variable-temperature cultivation. *Bioresour. Technol.* 239, 236–243.
- Shen, S., Wang, G., Zhang, M., Tang, Y., Gu, Y., Jiang, W., Wang, Y., Zhuang, Y., 2020. Effect of temperature and surfactant on biomass growth and higher-alcohol production during syngas fermentation by *Clostridium carboxidivorans* P7. *Bioresour. Bioprocess.* 7 (56).
- Shen, Y., Brown, R., Wen, Z., 2014. Syngas fermentation of *Clostridium carboxidivorans* P7 in a hollow fiber membrane biofilm reactor: Evaluating the mass transfer coefficient and ethanol production performance. *Biochem. Eng. J.* 85, 21–29.
- Shen, Y., Brown, R.C., Wen, Z., 2017b. Syngas fermentation by *Clostridium carboxidivorans* P7 in a horizontal rotating packed bed biofilm reactor with enhanced ethanol production. *Appl. Energy* 187, 585–594.
- Valgepea, K., de Souza Pinto Lemgruber, R., Abdalla, T., Binos, S., Takemori, N., Takemori, A., Tanaka, Y., Tappel, R., Köpke, M., Simpson, S.D., Nielsen, L.K., Marcellin, E., 2018. H₂ drives metabolic rearrangements in gas-fermenting *Clostridium autoethanogenum*. *Biotechnol. Biofuels* 11, 55.
- Valgepea, K., de Souza Pinto Lemgruber, P., Meaghan, K., Palfreyman, R.W., Abdalla, T., Heijstra, B.D., Behrendorf, J.B., Tappel, R., Köpke, M., Simpson, S.D., Nielsen, L.K., Marcellin, E., 2017. Maintenance of ATP Homeostasis triggers metabolic shifts in gas-fermenting acetogens. *Cell Syst.* 4 (5), 505–515.e5.
- Vees, C.A., Neundorff, C.S., Pflügl, S., 2020. Towards continuous industrial bioprocessing with solventogenic and acetogenic clostridia: challenges, progress and perspectives. *J. Ind. Microbiol. Biotechnol.* 47, 753–787.
- von Kamp, A., Thiele, S., Hädicke, O., Klamt, S., 2017. Use of *Cell NetAnalyzer* in biotechnology and metabolic engineering. *J. Biotechnol.* 261, 221–228.
- Wirth, S., Dürre, P., 2021. Investigation of putative genes for the production of medium-chained acids and alcohols in autotrophic acetogenic bacteria. *Metab. Eng.* 66, 296–307.
- Zhang, J., Taylor, S., Wang, Y., 2016. Effects of end products on fermentation profiles in *Clostridium carboxidivorans* P7 for syngas fermentation. *Bioresour. Technol.* 218, 1055–1063.